Accepted Manuscript

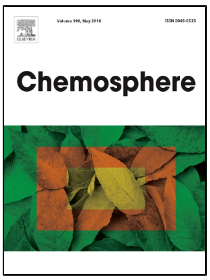

The characterization of γH2AX and p53 as biomarkers of genotoxic stress in a rainbow trout (*Oncorhynchus mykiss*) brain cell line

Mark E. Hamilton, Niels C. Bols, Bernard P. Duncker

PII:	S0045-6535(18)30420-X
DOI:	10.1016/j.chemosphere.2018.03.015
Reference:	CHEM 20959
To appear in:	*Chemosphere*
Received Date:	05 December 2017
Revised Date:	15 February 2018
Accepted Date:	03 March 2018

Please cite this article as: Mark E. Hamilton, Niels C. Bols, Bernard P. Duncker, The characterization of γH2AX and p53 as biomarkers of genotoxic stress in a rainbow trout (*Oncorhynchus mykiss*) brain cell line, *Chemosphere* (2018), doi: 10.1016/j.chemosphere. 2018.03.015

The characterization of γH2AX and p53 as biomarkers of genotoxic stress in a rainbow trout (*Oncorhynchus mykiss*) brain cell line

Mark E. Hamilton, Niels C. Bols, Bernard P. Duncker*.

Department of Biology, University of Waterloo, Waterloo, ON N2L 3G1, Canada

*Corresponding author. Tel.: +1 519 888 4567 ext. 33957

Email address: bduncker@uwaterloo.ca (B. P. Duncker)

ABSTRACT

Rainbow trout cell cultures were exposed to three genotoxicants and examined for effects on γH2AX and p53 levels by western blotting and on cell viability using the indicator dyes Alamar Blue (AB) for energy metabolism and 5'-carboxyfluorescein diacetate acetoxymethyl ester (CFDA-AM) for plasma membrane integrity. Bleomycin induced γH2AX and p53 in a dose- and time-dependent manner and had little cytotoxic effect. However, induction was first seen at 0.26 μM for γH2AX but not until 16.52 μM for p53. Methyl methanesulfonate (MMS) increased H2AX phosphorylation but diminished p53 levels as the dose was increased from 908 μM up to 2724 μM. Over this dose range cell viability was progressively lost. 4-nitroquinoline N-oxide (NQO) induced both γH2AX and p53, beginning at 62.5 nM, which was also the concentration at which cell viability began to decline. As the NQO concentration increased further, elevated γH2AX was detected at up to 2.00 μM, while p53 was elevated up to 1.00 μM. Therefore, H2AX phosphorylation was superior to p53 levels as a marker of DNA damage caused by genotoxicants that act by introducing double-stranded DNA breaks (bleomycin), alkyl groups (MMS), and quinoline adducts (NQO).

Key words: genotoxicity; cytotoxicity; γH2AX; p53; fish; cell lines

Abbreviations:

AB	Alamar Blue
CFDA-AM	5'-carboxyfluorescein diacetate acetoxymethyl ester
DDR	DNA damage response
DSB	Double-stranded break
MMS	Methyl methanesulfonate
NQO	4-nitroquinoline N-oxide
RT	Rainbow trout

1. INTRODUCTION

Rainbow trout (RT), *Oncorhynchus mykiss* (Walbum), and RT cell lines are increasingly being used to study and detect the genotoxicity of environmental contaminants and of commercial products that might reach the aquatic environment (Antunes et al., 2016; Capkin et al., 2017; Rodrigues et al., 2016; Vacchi et al., 2016; Zeng et al., 2016a). *O. mykiss* is used because the species is widely distributed, easily maintained in the laboratory, and has long been used in research, especially in toxicology (Wolf & Rumsey, 1985). RT cell lines have been developed from most tissues and organs of this species and are collectively referred to as the RT invitrome (Bols et al, 2017). Their experimental advantages include savings in cost and time, simplified design and dosing, and reducing the use of animals (Bols, 1991). In environmental

toxicology, they can be used to detect and rank toxicants and to identify and evaluate biomarkers (Bols et al., 2005; Schirmer, 2006). Biomarkers can be used *in vivo* to determine whether fish have been exposed to and impacted by a particular toxicant or toxicant class. For genotoxicants, biomarkers might be sought among the proteins involved in the DNA damage response (DDR), which is the collection of mechanisms for ameliorating DNA damage and involves proteins that detect DNA lesions, signal their presence, and promote their repair (Jackson & Baretek, 2009). However, relatively little is known about the DDR in RT cell lines. Two DDR proteins that might be used as biomarkers of genotoxicants are H2AX and p53.

H2AX is the X variant of histone 2A and undergoes phosphorylation in response to DNA damage (Fernandez-Capetillo et al. 2004), while p53 is a central regulatory protein of many fundamental activities including DNA repair (Vogelstein et al., 2000ab) and can accumulate in response to DNA-damaging agents (Fritsche et al., 1993). Upon the formation of double-stranded DNA breaks (DSB) via oxidative stress, replicative stress, enzyme activity, chemical exposure, or ionizing radiation, the Mre11-Rad50-Nbs1 (MRN) end-processing and sensor complex interacts with DNA proximal to the break through Rad50 (van den Bosch et al., 2003). Nbs1 is required in order to recruit Ataxia telangiectasia mutated (ATM) to lesions, while Mre11 possesses endonuclease activity (Ackermann & El-Deiry, 2008; Furuta et al., 2003; Stracker & Petrini, 2011; van den Bosch et al., 2003). ATM, a sensor of the phosphoinositide-3-kinase (PIKK) family, along with ataxia telangiectasia and Rad3-related (ATR) and the DNA protein kinase catalytic subunit (DNA-PK), phosphorylate Ser139 of mammalian H2AX in the C'-terminal SQ motif, and the result is commonly referred to as γH2AX (Rogakou et al., 1998; Shiloh, 2003). The regulation of p53 activity and expression is complex. Some post-translational

73 modifications include ubiquitylation, methylation, ADP-ribosylation, glycosylation,
74 SUMOylation (small ubiquitin-like modifiers), NEDDylation (neural precursor cell expressed,
75 developmentally down-regulated 8), acetylation, and phosphorylation at multiple sites
76 (Vogelstein et al., 2000b, Zhou et al., 2017). Although mammalian cell lines have been used
77 intensively to study H2AX and p53 regulation, the focus has most commonly been to understand
78 the development and treatment of tumors (Mantovani et al., 2017; Tran et al., 2017) rather than
79 for an environmental purpose. However, several human cell lines have shown to be useful for
80 assessing the genotoxicity of polycylic aromatic hydrocarbons (PAHs) (Audebert et al., 2010).
81
82 Relatively few studies have been done on H2AX and p53 in RT and RT cell lines. H2AX was
83 phosphorylated in fish after exposure to tritiated water (Festarini et al., 2016) and in the cell
84 lines, RTgill-W1 and RTH-149, upon exposure to cadmium (Krumschnabel et al., 2010). Thus,
85 γH2AX would appear to be a biomarker for DNA damage in RT but studies on more classical
86 DNA damaging agents would help to confirm a relationship. Studies on p53 in RT cell lines hint
87 at p53 behaving slightly differently in RT cells than in mammalian cells. Several DNA damaging
88 agents that induced p53 in mammalian cells failed to increase p53 levels in RTL-W1 (Embry et
89 al., 2006) and RTbrain-W1 (Liu et al., 2011). Also, two p53 inhibitors, 2-
90 phenylethynesulfonamide and pifithrin-α, had off-target actions on RTgill-W1 (Zeng et al.,
91 2014; 2016b). Thus, more studies are needed on H2AX and p53 in RT cell lines.
92
93 In the current study, changes in H2AX phosphorylation and p53 levels were investigated in
94 RTbrain-W1 in response to three model DNA-damaging compounds: bleomycin (BLEO),
95 methyl methanesulfonate (MMS), and 4-nitroquinoline N-oxide (NQO). Although the capacity

of this cell line for xenobiotic metabolism has yet to be explored, RTbrain-W1 was used because it has been characterized previously for expression of several genes in the DDR (Liu et al., 2011; Steinmoeller et al., 2009) and because recent mammalian research has shown surprising roles for the DDR in the brain. DNA repair is now being viewed as an essential part of brain physiology (Suberbielle et al., 2013) and alterations in DNA repair are associated with neurodegenerative diseases (Merlo et al., 2016) and stress (Hare et al., 2018). The compounds were chosen because their mode of genotoxicity is reasonably well known in yeast and in mammals. Bleomycin generates double-stranded breaks (DSBs) (Povirk, 1996) which are repaired by homologous recombination (HR) or non-homologous end joining depending on cell phase (Thompson, 2012). MMS monoalkylates DNA (Beranek, 1990; Ma et al., 2011), causing single-stranded breaks repaired by base excision (Pascucci et al., 2005), or HR upon replication-dependent double-stranded breaks (Nikolova et al., 2010). NQO metabolites form quinoline adducts (Galiègue-Zouitina et al., 1985; Kohda et al., 1991) that can be repaired by nucleotide excision repair (Snyderwine & Bohr, 1992), or when left unrepaired, leads to DSBs and chromosomal rearrangements (Brüsehafer et al., 2016). They were also chosen because their actions on mammalian cell lines have been intensively studied (Arima et al., 2006; Banáth & Olive, 2003; Khoury et al., 2016; Liu et al., 2014; Schroeder et al., 2014; Valentin-Severin et al., 2003; Wang et al., 2013). Our results showed that when RTbrain-W1 cells were exposed to these genotoxicants, γH2AX levels were elevated in a dose- and time-dependent fashion, suggesting that H2AX phosphorylation might be a good biomarker of genotoxicant exposure in rainbow trout.

2. MATERIALS AND METHODS

119 *2.1 Chemicals*

120 Biomarker testing was performed using methyl methanesulfonate (MMS; CAS 66-27- 3,
121 #129925), 4-Nitroquinoline *N*-oxide (NQO; CAS 56-57-5, #N8141), and bleocin (proprietary
122 name for bleomycin, referred to as BLEO; CAS 55658-47-4, #203408-M) that were all
123 purchased from Sigma-Aldrich. 4-NQO was dissolved in dimethyl sulfoxide (DMSO; CAS 67-
124 68-5, #472301) from Sigma-Aldrich for dosing. The final concentration of DMSO in media was
125 0.5% v/v, which is not cytotoxic on its own to cells (Schnell et al., 2009). BLEO and MMS were
126 dissolved in ultrapure deionized water for dosing, where the solvent never exceeded 1% of total
127 exposure volume. These solvents were used as mock-treated negative controls for exposure of
128 the respective chemicals they were used to dissolve.

129

130 *2.2 Cell cultures and exposure*

131 Testing was performed in an adherent glial cell line cultured from the brain of rainbow trout
132 (*Onchorhynchus mykiss*) named RTbrain-W1, which has seen limited use in the literature
133 (Fischer et al., 2011; Liu et al., 2011; Lončar et al., 2010; Steinmoeller et al., 2009; Vo et al.,
134 2015). Cells were routinely grown in 75 cm^2 (T75) polystyrene tissue culture flasks (BioLite,
135 Thermo Fisher Scientific) at room temperature (RT; 20 ± 2 °C) in L-15 basal medium (HyClone,
136 GE Healthcare) supplemented with 15% fetal bovine serum (FBS; Gibco, Thermo Fisher
137 Scientific) and a 1% penicillin-streptomycin cocktail (P/S; HyClone, GE Healthcare). Routine
138 passaging and seeding was performed using 0.25% v/v trypsin (HyClone, GE Healthcare) diluted
139 in Dulbecco's phosphate-buffered saline (DPBS; from HyClone, GE Healthcare), and cells were
140 used between their 5^{th} and 25^{th} passages.

141 Prior to exposing cells to genotoxicants or solvent only for controls, cells were removed from

142 T75s by trypsinization and centrifuged (3,000 RPM for 5 min at 18 °C). The trypsin was
143 removed, and cells were seeded on either a 96-well plate or a 6-well plate (BioLite, Fisher
144 Scientific) for cytotoxicity tests or western blots, respectively, in L-15 with 15% FBS and 1%
145 P/S for 24 h at RT. All genotoxicant exposures occurred in medium of L-15 with 10% FBS and
146 1% P/S.

147

148 *2.3 Cytotoxicity*

149 Cytotoxicity in cultures was evaluated through phase contrast microscopy observations and
150 the use of the two fluorescent indicator dyes, Alamar Blue (AB; Invitrogen) and 5-
151 carboxyfluorescein diacetate acetoxymethyl ester (CFDA-AM; CAS 124412-00-6, Sigma-
152 Aldrich). The microscopy approach had two particular strengths. The phase contrast observations
153 allowed cytotoxicity to be evaluated in the very same cultures that were actually going to be
154 analyzed by western blotting. They also indicated the exposure concentrations and times at
155 which cytotoxicity was just starting to be expressed, which was observed with cell rounding and
156 striation of cellular junctions, and at which cytotoxicity was complete, which was observed by
157 detachment of cells and the appearance of cellular debris. The indicator dyes provided
158 confirmation of these two extreme ends of the cytotoxicity responses and quantified cell viability
159 in cultures undergoing exposure conditions that elicit responses in between these two extremes.
160 The phase contrast observations were made on cultures in 6 to 8 independent experiments. The
161 indicator dyes were applied to cultures in 2 independent experiments.

162

163 The AB and CFDA-AM were applied to cultures in 96-well plates as described previously in

a step-by-step protocol (Dayeh et al., 2005, 2013). The AB stock solution comes in water, and was diluted in DPBS to form a working solution of 5% v/v, and the CFDA-AM was solubilized in DMSO to form a 4 mM stock, which was further diluted to a working solution of 4 μM. Both AB and CFDA-AM can be applied individually as outlined previously (Ganassin & Bols, 2000). However, in all experiments AB was combined with CFDA-AM so that the two different viability endpoints were simultaneously measurable on the same culture wells, as performed previously (Schirmer et al., 1997).

To prepare experiments, cells were trypsinized and removed from T75s as described above. Following centrifugation (3,000 RPM for 5 min at 18 °C) to remove trypsin, 200 μL of cells in growth medium were seeded on a 96-well multiplate at a density of $4x10^4$ cells per well. All wells were inoculated except the top row, which was to be kept void of cells as a zero during spectrophotometry for media containing genotoxicants. Plates were sealed in Parafilm and incubated in the dark at RT for 24 h. Once a dilution series of the genotoxicant to be tested was made and ready to be administered, the growth medium was aspirated and cells were treated with 200 μL of the genotoxicant dilution in described exposure medium, resealed, and incubated for 24 h in the dark at RT. The bottom row of the plate was not dosed, but rather left in original growth medium as an internal control to ensure that the mechanical effect of dosing had no significant impact on viability. Thus, 6 wells from each column were subjected to genotoxic challenge, with two columns set aside for a mock-treatment solvent control and a positive control for loss of viability, which was 4.54 mM MMS. The remaining 10 columns were challenged with various concentrations of the genotoxicant. Following 24 h exposure, the entire plate was aspirated, gently washed twice with DPBS and incubated with 100 μL of the working solution

for 1 h at RT in the dark. Relative fluorescent units (RFUs) of each well were then measured with a fluorescence multiplate reader, the CytoFluor 4000 (PerSeptive Biosystems). RFUs from the untreated and positive control rows were used for the experimenter's reference only, and were not included in calculations. The top row was averaged and subtracted from the mean of each treatment column in order to correct for background absorbance. The corrected mean values (n=6 per concentration) of the 10 experimentally treated columns were normalized to the mean corrected mock-treated control. RFUs were subjected to ANOVA, and when $p < 0.05$, the Dunnett multiple comparisons test was applied. Mean RFUs for each genotoxicant treatment were expressed as a percentage of the control RFUs and plotted as percent cell viability. The standard deviation of each mean was shown by error bars.

2.4 Cell lysis and protein extract preparation

After treatment, cells were washed with DPBS and scraped off the surface of 6-well plates. The cells were then centrifuged (3,000 RPM for 5 min at 4 °C) to remove the supernatant, and the pellet was lysed in ice-cold modified radioimmunoprecipitate assay (RIPA) buffer (50 mM HEPES-KOH, pH 7.5, 140 mM NaCl, 1 mM EDTA, 1% Triton X-100, 0.1% Na-deoxycholate) supplemented with Halt protease inhibitor (Roche). Cell debris was separated via centrifugation (14,800 RPM for 10 min at 4 °C) and protein concentration of each lysate supernatant was assayed by a bicinchoninic acid (BCA) kit (Pierce) using a VICTOR X3 1420 multilabel plate reader (PerkinElmer Inc.). Samples were kept on ice at all times.

2.5 Electrophoresis and Immunoblotting

Protein extracts were prepared for electrophoresis by addition of Laemmli buffer (0.0005% bromophenol blue, 10% glycerol, 2% SDS, 63 mM Tris-HCl, pH: 6.8) containing 0.1% β-mercaptoethanol and boiling for 10 min. After resting on ice, 50 µg aliquots of each sample were resolved in 12% polyacrylamide gels via SDS-PAGE using a Mini-Protean™ electrophoretic apparatus (Bio-Rad). Extracts were electrophoretically transferred to a 0.2 µm nitrocellulose membrane (Bio-Rad) using a Trans-Blot® Turbo™ semi-dry transfer system (Bio-Rad) and Bjerrum Schafer-Nielsen buffer (48 mM Tris, 39 mM glycine, 20% MeOH, pH: 9.2), and stained for extract quality and equal loading by Ponceau stain (Sigma). Blots were blocked in tris-buffered saline with Tween-20 (TBS-T; 136 mM NaCl, 2.68 mM KCl, 24.8 mM Tris base, 0.1% Tween-20) containing 5% bovine serum albumin (BSA, Sigma) for 1 h at RT with shaking or statically overnight at 4 °C.

Blots were then sequentially incubated with rabbit anti-β-actin polyclonal antibody (A2066, Sigma) at a 1:1,000 dilution in blocking buffer for 1 h at RT with shaking. After washing with TBS-T, blots were incubated with rabbit anti-γH2AX monoclonal antibody (9718, CellSignal) at a 1:1,000 dilution in blocking buffer overnight at 4 °C. The antibody specifically recognizes pSer139 of the H2AX C'-terminus, and not the unphosphorylated residue. After washing with TBS-T, blots were incubated overnight at 4 °C with rabbit anti-p53 polyclonal antibody (Liu et al., 2011) at a 1:1,000 dilution in blocking buffer. Finally, blots were washed with TBS-T and incubated for 1 h with a goat anti-rabbit secondary IgG antibody conjugated to horseradish peroxidase (HRP) (Bio-Rad) at a 1:5,000 dilution in TBS-T with 5% skim milk for 1 h at RT with shaking. Blots were washed in TBS-T and developed for 10 min in the dark with Clarity™ ECL substrate (Bio-Rad), and imaged using a ChemiDoc™ MP imaging system (Bio-Rad). Post-

image processing was performed using ImageLab™ software (Bio-Rad). All detections for each blot are from the same membrane (ie. p53, actin, γH2AX). In **Fig. 4**, antibody detections from low and high doses are from the same exposure, and were processed together.

2.6 Immunocytochemical staining of γH2AX

Cultures exposed to bleomycin were examined by immunocytochemistry for nuclear foci of γH2AX staining. This was done for γH2AX because as the research unfolded, this seemed to be the most promising biomarker and because bleomycin could be studied without the complications of cells dying in the cultures. Cells were suspended in growth medium at a density of $1x10^6$ cells/mL and 1 mL of the suspension was seeded into Nunc™ Lab-Tek™ slideflasks (Thermo Fisher Scientific), sealed with Parafilm, and allowed to adhere in the dark at RT for 24 h. One slideflask was dosed only with solvent (H_2O) to serve as a mock-treated control; a second received 1 mM H_2O_2 (Sigma-Aldrich) for 24 h at RT for the expected generation of foci as a positive control; and a third was set aside with no 1° antibody treatment to account for any background signal caused by non-specific binding of the 2° antibody. The remaining six flasks were dosed with 8.26 μM bleomycin, resealed with Parafilm, and incubated at RT in the dark until various time points. After exposure, medium was removed by aspiration and cells were gently rinsed twice with cold DPBS and fixed with paraformaldehyde (3% in DPBS) at 4 °C for 20 min, followed by permeabilization with 0.1% v/v Triton X-100 in DPBS for 10 min at RT. Slideflasks were then blocked overnight (3% v/v BSA, 10% v/v goat serum, 0.1% v/v Triton X-100; in DPBS) at 4 °C. After aspiration, 1° rabbit anti-γH2AX monoclonal antibody at a concentration of 1:1000 in the described blocking buffer was added to all slides except for 2° antibody control. Following 1 h incubation at RT with shaking, the wells were rinsed twice

and the 2° antibody, goat anti-rabbit AlexaFluor® 488 (Thermo Fisher Scientific) at a concentration of 1:8,000 in DPBS, was applied to all flasks. The slide was incubated at RT with shaking in the dark for 1 h prior to removal of unbound antibody by aspiration. The wells were rinsed twice and mounted with Fluoroshield™ (Thermo Fisher Scientific), which contains the nuclear stain DAPI (4′,6-Diamidine-2′-phenylindole dihydrochloride). Slides were left at RT in the dark for 24 h, and then examined with a Carl Zeiss LSM 700 confocal microscope. Post-image processing was performed using the supplied software, ZEN 2011. On three independent occasions, cultures that had been exposed to bleomycin were stained and viewed by confocal microscopy as described above. For one set of cultures, a scoring system was developed to illustrate how the γH2AX staining patterns of cultures might be quantified. The DAPI-stained nuclei were categorized into four types (A, B, C & D) based on a system that Festarini et al (2016) used for γH2AX detection of cell suspensions from rainbow trout. The precise definitions of the categories for RTbrain-W1 are given in the legend of **Fig. 5**.

3. RESULTS

3.1 Effect of NQO on cell viability

NQO exposures of 24 h caused a loss of cell viability in RTbrain-W1 cultures. Cells remained attached to the plastic surface and retained their bipolar morphology in cultures dosed with up to 500 nM NQO (**Fig. 1A**). At 1,000 nM NQO, many cells had rounded, and at higher concentrations most cells had completely detached. AB readings were significantly diminished at 62.5 nM NQO, while a decrease in CFDA-AM readings was not seen until 250 nM, suggesting again that the genotoxicant impaired energy metabolism before plasma membrane integrity (**Fig. 2A**). At the highest NQO concentrations (1,000 to 8,000 nM), neither AB nor CFDA-AM

readings were recorded because the detached and detaching cells had been removed with the medium changes necessary before the indicator dyes were added to the culture wells.

3.2 Effect of NQO on γH2AX and p53 levels

As evaluated by western blotting, the addition of NQO to RTbrain-W1 cultures increased γH2AX and p53 levels in a dose- and time-dependent manner (**Fig. 3A & 4A**). H2AX phosphorylation and elevated p53 levels were first noted at a concentration where energy metabolism began to be impaired, 62.5 nM (**Fig 2A**), and increased with increasing NQO concentrations up to 250 nM (**Fig. 3A**). At 1,000 and 4,000 nM NQO, the signals for p53 and γH2AX were completely lost, respectively (**Fig. 3A**). These were concentrations with no viable cells in the culture (**Fig. 2A**). As for time-dependent response, exposures to 250 nM NQO, a concentration that impaired energy metabolism (**Fig. 2A**), caused an elevation in p53 as early as 2 h after dosing and in H2AX phosphorylation after 12 h (**Fig. 4A**). However, with 1,000 nM NQO, H2AX phosphorylation was seen as early as 2 h after dosing, but p53 levels declined over time (**Fig. 4C**) as did cell viability. Therefore, both γH2AX and p53 induction appeared to indicate DNA damage by NQO but only as the cells began to die.

3.3 Effect of MMS on cell viability

MMS exposures of 24 h caused a loss of cell viability in RTbrain-W1 cultures. Cells rounded up but largely remained on the culture surface with 681 μM MMS (**Fig. 1B**). However, as the concentration was increased up to 2,724 μM, more cells completely detached from the surface (**Fig. 1B**). At 908 μM MMS, energy metabolism was impaired as evaluated with AB, whereas plasma membrane integrity as measured with CFDA-AM was unchanged (**Fig. 2B**), suggesting

that an impairment of energy metabolism is an early consequence of MMS exposure. At 1,589 μM and higher, plasma membrane integrity was compromised (**Fig. 2B**), with approximately an 80% decline at the highest MMS concentration, 2,497 μM.

3.4 Effect of MMS on γH2AX and p53 levels

The addition of MMS to RTbrain-W1 cultures increased H2AX phosphorylation in a dose-dependent manner but not p53 levels (**Fig. 3B**). Without any exposure to genotoxicants (ie. control cultures), no signal was seen for γH2AX (**Fig. 3B** & **4B**), while the p53 signal was usually faint (**Fig. 3B**). MMS at 908 μM was a pivotal concentration. This was the lowest concentration at which a consistent induction of γH2AX was detected (**Fig. 3B**) and at which a sign of cytotoxicity, a diminishment in AB readings, was observed (**Fig 2B**). As concentrations were increased above 908 μM, γH2AX signal became stronger while the p53 signal declined along with cell viability (**Fig. 3B**). The time course for H2AX phosphorylation began at 12 h and became stronger at 24 h (**Fig. 4B**). A time course for p53 was not systematically studied because a diminishment rather than an increase in levels of this protein was seen over 24 h (**Fig. 3B**). Therefore, only H2AX phosphorylation appeared to indicate DNA damage by MMS.

3.5 Effect of bleomycin on cell viability

Bleomycin had no apparent effects on the viability of RTbrain-W1 cells as judged by the appearance of cells under the phase contrast microscope and by the indicator dyes, AB for energy metabolism and CFDA-AM for plasma membrane integrity. In monolayer cultures that had been dosed at up to 264 μM of bleomycin, no changes in cellular morphology (**Fig. 1C**), energy metabolism, and plasma membrane integrity (**Fig. 2C**) were observed over 24 h of

exposure. The same results were obtained even when the concentration had been increased up to 5.29 mM.

3.6 Effect of bleomycin on γH2AX and p53 levels

As evaluated by western blotting, the addition of bleomycin to RTbrain-W1 cultures increased γH2AX and p53 levels in a manner that was dose- (**Fig. 3C**) and time-dependent (**Fig. 4C**). For dose, an increase in γH2AX was seen at concentrations as low as 0.26 μM, while the lowest concentration increasing p53 was 16.53 μM, approximately 60-fold higher. The highest bleomycin dose, 264.44 μM, elicited the strongest signal for both γH2AX and p53 (**Fig. 3C**). For time (**Fig. 4C**), γH2AX was elevated as early as 2 h of exposure, while p53 induction was first seen after a 12 h exposure.

Immunocytochemical staining of cultures for γH2AX revealed four types of nuclei (**Fig. 5A**). Nearly all the nuclei in control cultures had no γH2AX staining (**Fig. 5B**). After 2 h treatment with 8.26 μM bleomycin, three additional nuclear staining patterns were seen: some nuclei had a few intensely stained foci of γH2AX; others had too many foci to conveniently count; and in others the staining was so intense that the nuclei appeared completely stained (**Fig. 5A**). By 4 h, over 50% of the nuclei stained for γH2AX and this continued for up to 24 h. Therefore, γH2AX staining clearly indicated DNA damage in RTbrain-W1 cells 4 to 24 h after the addition of bleomycin**.**

4. DISCUSSION

346 H2AX phosphorylation was superior to p53 levels as a marker of DNA damage caused by the
347 model genotoxicants, especially for MMS and NQO. For MMS, γH2AX was induced in a dose-
348 dependent fashion but p53 levels declined as the dose increased. These contradictory responses
349 occurred at concentrations that were starting to impair cell viability. In these experiments all
350 cells in cultures, including detached, dead, and dying cells, were collected by low speed
351 centrifugation (3,000 RPM for 5 min at 4 °C) into a pellet that was processed for western
352 blotting. The nuclear chromatin location of γH2AX likely meant that all the γH2AX in cultures
353 was anchored in nuclei and collected in the pellets. By contrast, as a protein whose levels are
354 constantly being modulated by several different degradation mechanisms (Tsvetkov et al., 2010)
355 and as a protein that shuttles between the cytoplasm and nucleus (Saha et al., 2016), p53 in dead
356 and dying cells might be more rapidly degraded and/or more easily leak out of nuclei into the
357 supernatant, which was not analyzed in the current study. This could explain the concurrent
358 decline in p53 levels and cell viability as the MMS dose increased. For NQO, p53 was elevated
359 earlier than γH2AX but the concentration range that triggered H2AX phosphorylation was much
360 wider. As with MMS, the responses to NQO were seen as cultures started to show declines in
361 cell viability and so the problem of p53 being lost from dying and dead cells likely accounted for
362 γH2AX but not p53 being detected in cultures treated with 1,000 nM NQO. At higher
363 concentrations, the cell killing was likely so early in the 24 h exposure that the cells did not have
364 time to phosphorylate H2AX.
365
366 For bleomycin, both γH2AX and p53 were elevated. However, γH2AX was elevated at a dose
367 as low as 0.26 μM and with 132.22 μM as early as 2 h. By contrast 8.26 μM of bleomycin and a
368 12 h exposure was needed for p53 to be elevated. Also, a variable constitutive level of p53

369 protein was seen, making induction more difficult to detect and might explain the past failures to
370 see changes in p53 levels with bleomycin and fish cells in vitro (Embry et al., 2006; Liu et al.,
371 2011). Overall, from the perspectives of sensitivity and methodology γH2AX was a more robust
372 marker of DNA damage by the three test compounds.
373
374 NQO and MMS elicited DNA damage in RTbrain-W1, as judged by the phosphorylation of
375 H2AX, but over different concentration ranges. Of all the compounds, NQO induced γH2AX at
376 the lowest concentration, 62.5 nM. This was also the concentration at which NQO began to
377 impair cell viability as measured with Alamar Blue. At 2 μM NQO, γH2AX signal was still
378 detected but all the cells were dead by all measures of cell viability. For MMS, much higher
379 concentrations were needed. DNA damage, and concurrently an impairment in cell viability,
380 began at 908 μM, and continued up to 2,724 μM. In mammalian cells, the genotoxicity and
381 cytotoxicity of NQO and MMS have been compared on several occasions, and although the
382 exposures and endpoints have varied, several generalizations can be drawn. NQO is a more
383 potent genotoxicant and cytotoxicant than MMS, with NQO and MMS eliciting responses in the
384 micro- and milli-molar ranges, respectively (Valentin-Severin et al., 2003; Khoury et al., 2016).
385 Expression of phosphorylated H2AX has often been observed at concentrations where some
386 measure of cell viability declined (Banáth & Olive, 2003). For example, NQO and MMS
387 strongly induced γH2AX in cultures of human cell lines at concentrations where the relative cell
388 count declined (Khoury et al., 2016). Thus, both a DNA-alkylating (MMS) and an adduct-
389 inducing (NQO) genotoxicant caused DNA damage and cytotoxicity in the rainbow trout cells at
390 similar concentrations as in mammalian cells. However, bleomycin behaved differently in
391 RTbrain-W1.

392

393 Bleomycin caused DNA damage in the rainbow trout cells but was not cytotoxic. As judged
394 by H2AX phosphorylation in western blots, DNA damage occurred in RTbrain-W1 cells at
395 bleomycin concentrations from as low as 0.26 μM to as high as 5.29 mM, with slight or no
396 changes in cell viability. Bleomycin has been reported to induce H2AX phosphorylation in a
397 wide variety of mammalian cells (Banath & Olive, 2003; Liu et al., 2014; Tomilin et al., 2001;
398 Watters et al., 2009) and the common endpoint has been the appearance of γH2AX foci in nuclei
399 (Watters et al., 2009; Tomilin et al., 2001). In these mammalian cell studies, an increase in
400 H2AX phosphorylation has been seen at bleomycin concentrations as low as 0.07 – 0.7 μM
401 (Watters et al., 2009) and as high as 132.2 μM (Tomilin et al., 2001) and as early as 2 h after
402 exposure (Tomilin et al., 2001). RTbrain-W1 responded to similar concentrations and as quickly,
403 so the piscine and mammalian cells appear similarly sensitive to DNA damage by bleomycin. By
404 contrast, bleomycin at 16.53 μM and above is commonly found to be cytotoxic to mammalian
405 cells (Schroder et al., 2014), although under some circumstances bleomycin resistance has been
406 observed (Chen et al., 2012; Wang et al., 2013). In these circumstances, a reduction in
407 cytotoxicity has been attributed to culture conditions, such as hypoxia, to poor uptake, and to
408 metabolic inactivation (Sikic, 1986; Wang et al., 2013). These factors, acting independently or
409 together, could be contributing to the bleomycin resistance of rainbow trout cells.

410

411 NQO, bleomycin and MMS have been used occasionally by others to study genotoxic
412 endpoints in fish cells *in vitro* and briefly reviewing the results points to possible future research
413 directions in developing H2AX phosphorylation as a biomarker in ecotoxicology. The
414 genotoxicity of NQO has been studied with cell lines from goldfish (GEM 199) (Mitani et al.,

1983), fathead minnow (FHM) (Walton et al., 1983), and rainbow trout (RTG-2 and RTO) (Nehls & Segner, 2005; Walton et al., 1983) and with primary cultures from three different rainbow trout tissues (Walton et al., 1984). The genotoxic endpoints have been the comet assay (Nehls & Segner, 2005), the induction of oubain-resistant mutants (Mitani et al., 1983), and unscheduled DNA repair synthesis (UDS) (Walton et al., 1983; 1984). NQO caused neither mutation in GEM 199 (Mitani et al., 1983) nor UDS in primary intestinal cell cultures (Walton et al., 1984), but did elicit responses in the other experimental systems, with the magnitude being stronger in the cell lines than in the primary cultures (Walton et al., 1984). With respect to time and dose required to elicit a response, the most sensitive of these was the comet assay in RTG-2 (Nehls & Segner, 2005). By contrast, the phosphorylation of H2AX in RTbrain-W1 required a higher dose and longer exposure time. Differences in sensitivity might reflect differences in how the two cell lines metabolize NQO. This might be explored further with other rainbow trout cell lines, such as RTL-W1 and RTG-2, which in preliminary results responded like RTbrain-W1 to bleomycin with elevated γH2AX. Bleomycin and MMS have been studied less frequently with fish cells *in vitro*. Bleomycin caused UDS in rainbow trout hepatocytes that had been permeablized with lysolecithin but this treatment bypasses the normal route of genotoxicant uptake (Miller et al., 1989). MMS has been studied in a zebrafish cell line (ZF4) with the endpoint being genome-wide changes in transcription (Li et al., 2016). Over 6,000 differentially regulated genes were seen in ZF4 with MMS at a concentration and exposure time where H2AX phosphorylation was first detectable in RTbrain-W1. Thus, RNA sequencing would appear to be superior for detecting subtle/long term effects. The strength of γH2AX in fish cell lines might be that this biomarker could more easily be incorporated into protocols for high throughput screening (HTS) of environmental contaminants as have been described recently with a range of

mammalian cell lines (Graepel et al., 2017). As well as the western blotting and immunocytochemistry done here, the endpoint could also be evaluated by flow cytometry, which has been used successfully with fish cells (Stuart et al., 2016).

5. CONCLUSIONS

In summary, the in vitro experiments of the current study support the use of γH2AX as a biomarker of DNA damage in rainbow trout cell lines. Preliminary results show two other rainbow trout cell lines, RTL-W1 and RTgill-W1, responded to bleomycin similarly to RTbrain-W1. In future studies, one or more of these cell lines could be incorporated into protocols for high throughput screening (HTS) of environmental contaminants as have been described recently with a range of mammalian cell lines (Graepel et al., 2017). As well as providing predictive information on sets of chemicals, such protocols could establish γH2AX as a genotoxicity marker in fish. The endpoints could include western blotting or immunohistochemistry as done here but another one could be flow cytometry, which has been used successfully with fish cells (Stuart et al., 2016). Additionally, the strong induction of γH2AX without cytotoxicity by bleomycin should make bleomycin/rainbow trout cell lines a good *in vitro* system for exploring other participants in the DDR and to develop them as additional biomarkers for environmental genotoxicants.

Acknowledgement

This research was supported by Natural Sciences and Engineering Research Council of Canada (NSERC) in the form of Discovery grants to NCB and BPD.

Conflict of Interest

None.

References

Ackermann, J.M., El-Deiry, W.S., 2008. ATM and ATR are Key Mediators of the DNA Damage Response Pathway, in: Dai, W. (Ed.), Checkpoint Responses in Cancer Therapy. Humana, Tuxedo, NY, pp. 93–116.

Antunes, S.C., Nunes, B., Rodrigues, S., Nunes, R., Fernandes, J., Correia, A.T., 2016. Effects of chronic exposure to benzalkonium chloride in Oncorhynchus mykiss: Cholinergic neurotoxicity, oxidative stress, peroxidative damage and genotoxicity. Environ. Toxicol. Pharmacol. 45, 115–122. https://doi.org/10.1016/j.etap.2016.04.016

Arima, Y., Nishigori, C., Takeuchi, T., Oka, S., Morimoto, K., Utani, A., Miyachi, Y., 2006. 4-Nitroquinoline 1-oxide forms 8-hydroxydeoxyguanosine in human fibroblasts through reactive oxygen species. Toxicol. Sci. 91, 382–392. https://doi.org/10.1093/toxsci/kfj161

Audebert, M., Riu, A., Jacques, C., Hillenweck, A., Jamin, E. L., Zalko, D., & Cravedi, J. P. (2010). Use of the γH2AX assay for assessing the genotoxicity of polycyclic aromatic hydrocarbons in human cell lines. *Toxicology letters*, *199*(2), 182-192.

Banáth, J.P., Olive, P.L., 2003. Expression of Phosphorylated Histone H2AX as a Surrogate of Cell Killing by Drugs That Create DNA Double-Strand Breaks. Cancer Res. 63, 4347–4350.

Beranek, D.T., 1990. Distribution of methyl and ethyl adducts following alkylation with monofunctional alkylating agents. Mutat. Res. - Fundam. Mol. Mech. Mutagen. 231, 11–30. https://doi.org/10.1016/0027-5107(90)90173-2

Bols, N.C., Pham, P.H., Dayeh, V.R., Lee, L.E.J., 2017. Invitromatics, invitrome, and invitroomics: introduction of three new terms for in vitro biology and illustration of their use with the cell lines from rainbow trout. Vitr. Cell. Dev. Biol. - Anim. https://doi.org/10.1007/s11626-017-0142-5

Bols, N.C., Dayeh, V.R., Lee, L.E.J., Schirmer, K., 2005. Use of fish cell lines in the toxicology and ecotoxicology of fish. Piscine cell lines in environmental toxicology, in: Mommsen, T.P., Moon, T.W. (Eds.), Biochemistry & Molecular Biology of Fishes. Elsevier, pp. 43–84. https://doi.org/10.1016/S1873-0140(05)80005-0

Bols, N.C., 1991. Biotechnology and aquaculture: The role of cell cultures. Biotechnol. Adv. https://doi.org/10.1016/0734-9750(91)90403-I

Brüsehafer, K., Manshian, B.B., Doherty, A.T., Zaïr, Z.M., Johnson, G.E., Doak, S.H., Jenkins, G.J.S., 2016. The clastogenicity of 4NQO is cell-type dependent and linked to cytotoxicity, length of exposure and p53 proficiency. Mutagenesis 31, 171–180. https://doi.org/10.1093/mutage/gev069

Capkin, E., Ozcelep, T., Kayis, S., Altinok, I., 2017. Antimicrobial agents, triclosan, chloroxylenol, methylisothiazolinone and borax, used in cleaning had genotoxic and

histopathologic effects on rainbow trout. Chemosphere 182, 720–729. https://doi.org/10.1016/j.chemosphere.2017.05.093

Chen, J., Chen, Y., He, Q., 2012. Action of bleomycin is affected by bleomycin hydrolase but not by caveolin-1. Int. J. Oncol. 41, 2245–2252. https://doi.org/10.3892/ijo.2012.1668

Dayeh, V.R., Bols, N.C., Tanneberger, K., Schirmer, K., Lee, L.E.J., 2013. The use of fish-derived cell lines for investigation of environmental contaminants: an update following OECD's fish toxicity testing framework No. 171. (No. Supplement 56), Current Protocols in Toxicology, Toxicological Models. John Wiley & Sons, Inc. https://doi.org/10.1002/0471140856.tx0105s56

Dayeh, V.R., Schrmer, K., Lee, L.E.J., Bols, N.C., Schirmer, K., Lee, L.E.J., Bols, N.C., 2005. Rainbow trout gill cell line microplate cytotoxicity test. Small-scale Freshw. Toxic. Investig. 1, 473–503. https://doi.org/10.1007/1-4020-3120-3_16

Embry, M., Billiard, S., Di Giulio, R., 2006. Lack of p53 induction in fish cells by model chemotherapeutics. Oncogene 25, 2004–2010. https://doi.org/10.1038/sj.onc

Fernandez-Capetillo, O., Lee, A., Nussenzweig, M., Nussenzweig, A., 2004. H2AX: the histone guardian of the genome. DNA Repair (Amst). 3, 959–967. https://doi.org/10.1016/j.dnarep.2004.03.024

Festarini, A., Shultz, C., Stuart, M., Kim, S.B., Ferreri, C., 2016. Cellular Responses to Tritium Exposure in Rainbow Trout: HTO- and OBT-spiked Feed Exposure Experiments. CNL Nucl. Rev. 5, 155–172. https://doi.org/10.12943/CNR.2015.00059

Fischer, S., Lončar, J., Zaja, R., Schnell, S., Schirmer, K., Smital, T., Luckenbach, T., 2011. Constitutive mRNA expression and protein activity levels of nine ABC efflux transporters in seven permanent cell lines derived from different tissues of rainbow trout (Oncorhynchus mykiss). Aquat. Toxicol. 101, 438–446. https://doi.org/10.1016/j.aquatox.2010.11.010

Furuta, T., Takemura, H., Liao, Z.Y., Aune, G.J., Redon, C., Sedelnikova, O.A., Pilch, D.R., Rogakou, E.P., Celeste, A., Chen, H.-T., Nussenzweig, A., Aladjem, M.I., Bonner, W.M., Pommier, Y., 2003. Phosphorylation of histone H2AX and activation of Mre11, Rad50, and Nbs1 in response to replication-dependent DNA double-strand breaks induced by mammalian DNA topoisomerase I cleavage complexes. J. Biol. Chem. 278, 20303–20312. https://doi.org/10.1074/jbc.M300198200

Galiègue-Zouitina, S., Bailleul, B., Loucheux-Lefebvre, M.H., 1985. Adducts from in vivo action of the carcinogen 4-hydroxyaminoquinoline 1-oxide in rats and from in vitro reaction of 4-acetoxyaminoquinoline 1-oxide with DNA and polynucleotides. Cancer Res. 45, 520–5.

Ganassin, R.C., Bols, N.C., 2000. Growth of rainbow trout hemopoietic cells in methylcellulose and methods of monitoring their proliferative response in this matrix. Methods Cell Sci. 22, 147–152. https://doi.org/10.1023/A:1009835814441

536 Graepel, R., Lamon, L., Asturiol, D., Berggren, E., Joossens, E., Paini, A., ... & Worth, A.
537 (2017). The virtual cell based assay: Current status and future perspectives. *Toxicology in*
538 *Vitro*, *45*, 258-267.
539
540 Hare, B. D., Thornton, T. M., Rincon, M., Golijanin, B., King, S. B., Jaworski, D. M., & Falls,
541 W. A. (2018). Two weeks of variable stress increases gamma-H2AX levels in the mouse bed
542 nucleus of the stria terminalis. *Neuroscience*.

543 Jackson, S.P., Bartek, J., 2009. The DNA-damage response in human biology and disease.
544 Nature. https://doi.org/10.1038/nature08467

545 Khoury, L., Zalko, D., Audebert, M., 2016. Evaluation of four human cell lines with distinct
546 biotransformation properties for genotoxic screening. Mutagenesis 31, 83–96.
547 https://doi.org/10.1093/mutage/gev058

548 Kohda, K., Kawazoe, Y., Minoura, Y., Tada, M., 1991. Separation and identification of N4-
549 (guanosin-7-yl)-4-aminoquinoline 1-oxide, a novel nucleic acid adduct of carcinogen 4-
550 nitroquinoline 1-oxide. Carcinogenesis 12, 1523–5.

551 Krumschnabel, G., Ebner, H.L., Hess, M.W., Villunger, A., 2010. Apoptosis and necroptosis are
552 induced in rainbow trout cell lines exposed to cadmium. Aquat. Toxicol. 99, 73–85.
553 https://doi.org/10.1016/j.aquatox.2010.04.005

554 Li, Z., Long, Y., Zhong, L., Song, G., Zhang, X., Yuan, L., & Dai, H. (2016). RNA sequencing
555 provides insights into the toxicogenomic response of ZF4 cells to methyl
556 methanesulfonate. *Journal of Applied Toxicology*, *36*(1), 94-104.
557

558 Liu, M., Hales, B.F., Robaire, B., 2014. Effects of Four Chemotherapeutic Agents, Bleomycin,
559 Etoposide, Cisplatin, and Cyclophosphamide, on DNA Damage and Telomeres in a Mouse
560 Spermatogonial Cell Line1. Biol. Reprod. 90. https://doi.org/10.1095/biolreprod.114.117754

561 Liu, M., Tee, C., Zeng, F., Sherry, J.P., Dixon, B., Bols, N.C., Duncker, B.P., 2011.
562 Characterization of p53 expression in rainbow trout. Comp. Biochem. Physiol. Part C
563 Toxicol. Pharmacol. 154, 326–32. https://doi.org/10.1016/j.cbpc.2011.06.018

564 Lončar, J., Popovic, M., Zaja, R., Smital, T., 2010. Gene expression analysis of the ABC efflux
565 transporters in rainbow trout (Oncorhynchus mykiss). Comp. Biochem. Physiol. Part C
566 Toxicol. Pharmacol. 151, 209–215. https://doi.org/10.1016/j.cbpc.2009.10.009

567 Ma, W., Westmoreland, J.W., Gordenin, D.A., Resnick, M.A., 2011. Alkylation base damage is
568 converted into repairable double-strand breaks and complex intermediates in g2 cells lacking
569 ap endonuclease. PLoS Genet. 7. https://doi.org/10.1371/journal.pgen.1002059

570 Mantovani, F., Walerych, D., & Sal, G. D. (2017). Targeting mutant p53 in cancer: a long road
571 to precision therapy. *The FEBS journal*, *284*(6), 837-850.

572
573 Merlo, D., Mollinari, C., Racaniello, M., Garaci, E., & Cardinale, A. (2016). DNA double strand
574 breaks: a common theme in neurodegenerative diseases. *Current Alzheimer*
575 *Research*, *13*(11), 1208-1218.
576
577 Miller, M. R., Blair, J. B., & Hinton, D. E. (1989). DNA repair synthesis in isolated rainbow
578 trout liver cells. *Carcinogenesis*, *10*(6), 995-1001.
579
580 Mitani, H. (1983). Lethal and mutagenic effects of radiation and chemicals on cultured fish cells
581 derived from the erythrophoroma of goldfish (Carassius auratus). *Mutation*
582 *Research/Fundamental and Molecular Mechanisms of Mutagenesis*, *107*(2), 279-288.
583
584 Nehls, S., & Segner, H. (2005). Comet assay with the fish cell line rainbow trout gonad-2 for in
585 vitro genotoxicity testing of xenobiotics and surface waters. *Environmental toxicology and*
586 *chemistry*, *24*(8), 2078-2087.
587
588 Nikolova, T., Ensminger, M., Löbrich, M., Kaina, B., 2010. Homologous recombination protects
589 mammalian cells from replication-associated DNA double-strand breaks arising in response
590 to methyl methanesulfonate. DNA Repair (Amst). 9, 1050–1063.
591 https://doi.org/10.1016/J.DNAREP.2010.07.005

592 Pascucci, B., Russo, M.T., Crescenzi, M., Bignami, M., Dogliotti, E., 2005. The accumulation of
593 MMS-induced single strand breaks in G1 phase is recombinogenic in DNA polymerase β
594 defective mammalian cells. Nucleic Acids Res. 33, 280–288.
595 https://doi.org/10.1093/nar/gki168

596 Povirk, L.F., Finley Austin, M.J., 1991. Genotoxicity of bleomycin. Mutat. Res. Genet. Toxicol.
597 https://doi.org/10.1016/0165-1110(91)90022-N

598 Rodrigues, R.M., Heymans, A., De Boe, V., Sachinidis, A., Chaudhari, U., Govaere, O.,
599 Roskams, T., Vanhaecke, T., Rogiers, V., De Kock, J., 2016. Toxicogenomics-based
600 prediction of acetaminophen-induced liver injury using human hepatic cell systems. Toxicol.
601 Lett. 240, 50–59. https://doi.org/10.1016/j.toxlet.2015.10.014

602 Rogakou, E.P., Pilch, D.R., Orr, A.H., Ivanova, V.S., Bonner, W.M., 1998. DNA double-
603 stranded breaks induce histone H2AX phosphorylation on serine 139. J. Biol. Chem. 273,
604 5858–5868. https://doi.org/10.1074/jbc.273.10.5858

605 Saha, T., Guha, D., Manna, A., Panda, A.K., Bhat, J., Chatterjee, S., Sa, G., 2016. G-actin guides
606 p53 nuclear transport: Potential contribution of monomeric actin in altered localization of
607 mutant p53. Sci. Rep. 6. https://doi.org/10.1038/srep32626

608 Schirmer, K., 2006. Proposal to improve vertebrate cell cultures to establish them as substitutes
609 for the regulatory testing of chemicals and effluents using fish. Toxicology 224, 163–183.
610 https://doi.org/10.1016/j.tox.2006.04.042

611 Schirmer, K., Chan, A.G.J., Greenberg, B.M., Dixon, D.G., Bols, N.C., 1997. Methodology for
612 demonstrating and measuring the photocytotoxicity of fluoranthene to fish cells in culture.
613 Toxicol. Vitr. 11, 107–119. https://doi.org/10.1016/S0887-2333(97)00002-7

614 Schnell, S., Kawano, A., Porte, C., Lee, L.E.J., Bols, N.C., 2009. Effects of Lbuprofen on the
615 viability and proliferation of rainbow trout liver cell lines and potential problems and
616 interactions in effects assessment. Environ. Toxicol. 24, 157–165.
617 https://doi.org/10.1002/tox.20410

618 Schroeder, B.R., Ghare, M.I., Bhattacharya, C., Paul, R., Yu, Z., Zaleski, P.A., Bozeman, T.C.,
619 Rishel, M.J., Hecht, S.M., 2014. The disaccharide moiety of bleomycin facilitates uptake by
620 cancer cells. J. Am. Chem. Soc. 136, 13641–13656. https://doi.org/10.1021/ja507255g

621 Shiloh, Y., 2003. ATM and related protein kinases: safeguarding genome integrity. Nat. Rev.
622 Cancer 3, 155–168. https://doi.org/10.1038/nrc1011

623 Sikic, B.I., 1986. Biochemical and cellular determinants of bleomycin cytotoxicity. Cancer Surv.
624 5, 81–91.

625 Snyderwine, E. G., & Bohr, V. A. (1992). Gene- and strand-specific damage and repair in
626 Chinese hamster ovary cells treated with 4-nitroquinoline 1-oxide. *Cancer research*, *52*(15),
627 4183-4189.
628
629 Steinmoeller, J. D., Fujiki, K., Arya, A., Müller, K. M., Bols, N. C., Dixon, B., & Duncker, B. P.
630 (2009). Characterization of rainbow trout CHK2 and its potential as a genotoxicity
631 biomarker. *Comparative Biochemistry and Physiology Part C: Toxicology &*
632 *Pharmacology*, *149*(4), 491-499.

633 Stracker, T.H., Petrini, J.H.J., 2011. The MRE11 complex: starting from the ends. Nat. Rev. Mol.
634 Cell Biol. 12, 90–103. https://doi.org/10.1038/nrm3047

635 Stuart, M., Festarini, A., Schleicher, K., Tan, E., Kim, S.B., Wen, K., Gawlik, J., Ulsh, B., 2016.
636 Biological effects of tritium on fish cells in the concentration range of international drinking
637 water standards. Int. J. Radiat. Biol. 92, 563–571.
638 https://doi.org/10.1080/09553002.2016.1222090

639 Suberbielle, E., Sanchez, P. E., Kravitz, A. V., Wang, X., Ho, K., Eilertson, K., ... & Mucke, L.
640 (2013). Physiologic brain activity causes DNA double-strand breaks in neurons, with
641 exacerbation by amyloid-β. *Nature neuroscience*, *16*(5), 613.

642 Thompson, L.H., 2012. Recognition, signaling, and repair of DNA double-strand breaks
643 produced by ionizing radiation in mammalian cells: The molecular choreography. Mutat.
644 Res. - Rev. Mutat. Res. https://doi.org/10.1016/j.mrrev.2012.06.002

645 Tomilin, N. V, Solovjeva, L. V, Svetlova, M.P., Pleskach, N.M., Zalenskaya, I. a, Yau, P.M.,
646 Bradbury, E.M., 2001. Visualization of focal nuclear sites of DNA repair synthesis induced

by bleomycin in human cells. Radiat. Res. 156, 347–354. https://doi.org/10.1667/0033-7587(2001)156[0347:VOFNSO]2.0.CO;2

Tran, T. Q., Gabra, M. B. I., Lowman, X. H., Yang, Y., Reid, M. A., Pan, M., ... & Kong, M. (2017). Glutamine deficiency induces DNA alkylation damage and sensitizes cancer cells to alkylating agents through inhibition of ALKBH enzymes. *PLoS biology*, *15*(11), e2002810.

Tsvetkov, P., Reuven, N., Shaul, Y., 2010. Ubiquitin-independent p53 proteasomal degradation. Cell Death Differ. https://doi.org/10.1038/cdd.2009.67

Vacchi, F.I., Vendemiatti, J.A.S., Brosselin, V., Ferreira da Silva, B., Maria, M.V., DeMeo, M., Bony, S., Devaux, A., Umbuzeiro, G.A., 2016. Combining different assays and chemical analysis to characterize the genotoxicity of waters impacted by textile discharges. Environ. Mol. Mutagen. 57, 559–571. https://doi.org/10.1002/em.22034

van den Bosch, M., Bree, R.T., Lowndes, N.F., 2003. The MRN complex: Coordinating and mediating the response to broken chromosomes. EMBO Rep. https://doi.org/10.1038/sj.embor.embor925

Valentin-Severin, I., Le Hegarat, L., Lhuguenot, J.-C., Le Bon, A.-M., Chagnon, M.-C., 2003. Use of HepG2 cell line for direct or indirect mutagens screening: comparative investigation between comet and micronucleus assays. Mutat. Res. Toxicol. Environ. Mutagen. 536, 79–90. https://doi.org/10.1016/S1383-5718(03)00031-7

Vo, N.T.K., Mikhaeil, M.S., Lee, L.E.J., Pham, P.H., Bols, N.C., 2015. Senescence-associated β-galactosidase staining in fish cell lines and primary cultures from several tissues and species, including rainbow trout coelomic fluid and milt. Vitr. Cell. Dev. Biol. - Anim. 51, 361–371. https://doi.org/10.1007/s11626-014-9837-z

Vogelstein, B., Lane, D., Levine, A.J., 2000a. p53: The most frequently altered gene in human cancers. Nature 408, 307–310.

Vogelstein, B., Lane, D., Levine, A.J., 2000b. Surfing the p53 network. Nature 408, 307–310. https://doi.org/10.1038/35042675

Walton, D. G., Acton, A. B., & Stich, H. F. (1983). DNA repair synthesis in cultured mammalian and fish cells following exposure to chemical mutagens. *Mutation Research/Genetic Toxicology*, *124*(2), 153-161.

Walton, D. G., Acton, A. B., & Stich, H. F. (1984). DNA repair synthesis following exposure to chemical mutagens in primary liver, stomach, and intestinal cells isolated from rainbow trout. *Cancer research*, *44*(3), 1120-1121.

Wang, Q., Cui, K., Espin-Garcia, O., Cheng, D., Qiu, X., Chen, Z., Moore, M., Bristow, R.G., Xu, W., Der, S., Liu, G., 2013. Resistance to bleomycin in cancer cell lines is characterized

682 by prolonged doubling time, reduced DNA damage and evasion of G2/M arrest and
683 apoptosis. PLoS One 8, e82363. https://doi.org/10.1371/journal.pone.0082363

684 Watters, G.P., Smart, D.J., Harvey, J.S., Austin, C.A., 2009. H2AX phosphorylation as a
685 genotoxicity endpoint. Mutat. Res. 679, 50–8.
686 https://doi.org/10.1016/j.mrgentox.2009.07.007

687 Wolf, K., Rumsey, G., 1985. The Representative Research Animal: Why Rainbow Trout (Salmo
688 gairdneri Rich.)? J. Appl. Ichthyol. 1, 131–138. https://doi.org/10.1111/j.1439-
689 0426.1985.tb00422.x

690 Zeng, F., Sherry, J.P., Bols, N.C., 2016a. Evaluating the toxic potential of benzothiazoles with
691 the rainbow trout cell lines, RTgill-W1 and RTL-W1. Chemosphere 155, 308–318.
692 https://doi.org/10.1016/j.chemosphere.2016.04.079

693 Zeng, F., Tee, C., Liu, M., Sherry, J.P., Dixon, B., Duncker, B.P., Bols, N.C., 2014. The
694 p53/HSP70 inhibitor, 2-phenylethynesulfonamide, causes oxidative stress, unfolded protein
695 response and apoptosis in rainbow trout cells. Aquat. Toxicol. 146, 45–51.
696 https://doi.org/10.1016/j.aquatox.2013.10.026

697 Zeng, F., Yu, X., Sherry, J.P., Dixon, B., Duncker, B.P., Bols, N.C., 2016b. The p53 inhibitor,
698 pifithrin-a, disrupts microtubule organization, arrests growth, and induces polyploidy in the
699 rainbow trout gill cell line, RTgill-W1. Comp. Biochem. Physiol. Part C Toxicol.
700 Pharmacol. 179, 1–10. https://doi.org/10.1016/j.cbpc.2015.08.002

701 Zhou, X., Cao, B., Lu, H., 2017. Negative auto-regulators trap p53 in their web. J. Mol. Cell
702 Biol. https://doi.org/10.1093/jmcb/mjx001

Figure Legends

Figure 1: Phase contrast microscopy of RTbrain-W1 cells treated with genotoxicants for 24 h.
Phase contrast micrographs illustrate the appearance of cells 24 RTbrain-W1 after exposure to NQO (**A**), MMS (**B**), and bleomycin (**C**). Images taken at 400X magnification. Scale bar represents 200 μm.

Figure 2: Effect of genotoxicants on cell viability in RTbrain-W1 cultures.
Cultures in 96-well plates were exposed to increasing concentrations of 4-nitroquinoline N-oxide (NQO) (**A**), methyl methanesulfonate (MMS) (**B**) and bleomycin (**C**). After 24 h of genotoxicant or solvent-only (control) exposure, cells were monitored with the fluorescent indicator dyes, Alamar Blue (AB; blue squares) for energy metabolism and 5-carboxyfluorescein diacetate acetoxymethyl ester (CFDA-AM; red triangles) for plasma membrane integrity. Results were recorded as RFUs, and the means of each concentration (n=6) were normalized and expressed as a percent of the control. Standard deviation is shown by error bars. Significant differences ($p < 0.05$) from the control are indicated with brackets under asterisks: for AB, a blue bar (upper) and for CFDA-AM, a red bar (lower). For panel C, AB at the highest bleomycin concentration is the only significantly different value from the control.

Figure 3: Effect of increasing concentration on γH2AX and p53 levels in RTbrain-W1 cells treated with genotoxicants for 24 h.
RTbrain-W1 cultures were exposed to NQO (**A**) MMS (**B**), or bleomycin (**C**) and analyzed for γH2AX and p53 induction after 24 h. Protein extracts were subjected to SDS-PAGE electrophoresis and western blotting. Ponceau S staining of protein extracts for quality and loading is shown at the top of the figures followed by detection of γH2AX, p53, and actin. The primary antibodies used were a rabbit anti-β-actin polyclonal antibody (A2066, Sigma), a rabbit anti-γH2AX monoclonal antibody (9718, Cell Signal), and a rabbit anti-p53 polyclonal antibody made in-house. The secondary antibody used was an HRP-conjugated goat anti-rabbit IgG. Each blot represents one of two independent trials.

Figure 4: Effect of increasing exposure times on γH2AX and p53 levels in RTbrain-W1 cells treated with genotoxicants.
RTbrain-W1 cultures were exposed to NQO (**A**) MMS (**B**), or bleomycin (**C**) at low or high concentrations and analyzed for γH2AX and p53 induction at various time points up to 24 h. Protein extracts were subjected to SDS-PAGE electrophoresis and western blotting. Ponceau S staining of protein extracts for quality and loading is shown at the top of the figures followed by detection of γH2AX, p53, and actin. The primary antibodies used were a rabbit anti-β-actin polyclonal antibody (A2066, Sigma), a rabbit anti-γH2AX monoclonal antibody (9718, Cell Signal), and a rabbit anti-p53 polyclonal antibody made in-house. The secondary antibody used was an HRP-conjugated goat anti-rabbit IgG. Each blot represents one of two independent trials. Antibody detections from low and high doses are from the same exposure, and were processed together.

Figure 5: Categorization of nuclear γH2AX staining after various time points in RTbrain-W1 cultures exposed to bleomycin.

After incubation with 8.26 mM bleomycin for up to 24 h, cultures were fixed immediately (0h), or after 2, 4, 12, or 24 h, and probed immunocytochemically for γH2AX (red) and counter-stained with DAPI (blue). Cultures were then placed into four categories (A, B, C and D) based on the intensity of their nuclear γH2AX staining pattern (**A**). The percentage of nuclei at each time point in each category is shown graphically (**B**). Category A had no staining. For category B, the nuclei had 1 to 8 γH2AX foci. Category C had more than 8 distinct γH2AX foci. The γH2AX staining was too intense to identify individual foci in category D. Scale bar represents 3 μm.

HIGHLIGHTS

- Three genotoxicants were studied on rainbow trout cells *in vitro*.
- Methyl methanesulfonate induced γH2AX but not p53.
- 4-nitroquinoline *N*-oxide induced both γH2AX and p53.
- Bleomycin induced γH2AX and p53, but γH2AX was more sensitive.